

A general framework for boundary equilibrium bifurcations of Filippov systems.

D.J.W. Simpson

Institute of Fundamental Sciences
Massey University
Palmerston North
New Zealand

May 1, 2018

Abstract

As parameters are varied a boundary equilibrium bifurcation (BEB) occurs when an equilibrium collides with a discontinuity surface in a piecewise-smooth system of ODEs. Under certain genericity conditions, at a BEB the equilibrium either transitions to a pseudo-equilibrium (on the discontinuity surface) or collides and annihilates with a coexisting pseudo-equilibrium. These two scenarios are distinguished by the sign of a certain inner product. Here it is shown that this sign can be determined from the number of unstable directions associated with the two equilibria by using techniques developed by Feigin. A new normal form is proposed for BEBs in systems of any number of dimensions. The normal form involves a companion matrix, as does the leading order sliding dynamics, and so the connection to the stability of the equilibria is explicit. In two dimensions the parameters of the normal form distinguish, in a simple way, the eight topologically distinct cases for the generic local dynamics at a BEB. A numerical exploration in three dimensions reveals that BEBs can create multiple attractors and chaotic attractors, and that the equilibrium at the BEB can be unstable even if both equilibria are stable. The developments presented here stem from seemingly unutilised similarities between BEBs in discontinuous systems (specifically Filippov systems as studied here) and BEBs in continuous systems for which analogous results are, to date, more advanced.

1 Introduction

The phase space of a Filippov system is divided into regions Ω_i within which evolution is governed by a smooth set of ODEs. Boundaries between regions, termed *discontinuity surfaces*, are assumed to be codimension-one and smooth (or possibly piecewise-smooth).

When an orbit reaches a discontinuity surface (as we follow it with increasing time), there are two generic possibilities for its subsequent motion: crossing and sliding. To be more precise, suppose the orbit resides in Ω_1 until reaching a discontinuity surface Σ bounding Ω_1 and Ω_2 . If the system in Ω_2 points away from Σ , as in Fig. 1-A, then the orbit *crosses* Σ and enters Ω_2 . Alternatively if the system in Ω_2 points towards the discontinuity surface, as in Fig. 1-B, then the orbit subsequently *slides* on Σ . Such sliding motion is governed by a convex combination of the systems in Ω_1 and Ω_2 .

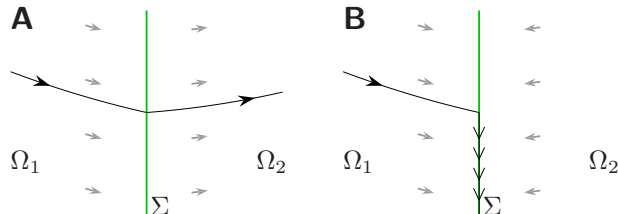


Figure 1: Sketches of an orbit of a Filippov system crossing a discontinuity surface (in panel A) and sliding on the discontinuity surface (in panel B).

In mathematical models, sliding motion usually has important physical interpretations. For instance in simple models of mechanical systems with stick-slip friction, sliding motion corresponds to the sticking phase of motion [1]. For relay control systems, sliding motion represents the idealised limit that the time between switching events is zero [2]. In an ecological model of Dercole *et. al.* [3], sliding motion corresponds to predators that are hesitating between two sources of food.

As parameters are varied, an equilibrium of a Filippov system can collide with a discontinuity surface. Such BEBs have been identified in mathematical models of a wide variety of physical systems, see for instance [4, 5, 6, 7]. Various invariant sets (such as limit cycles) can be created in BEBs. But if we look only at equilibria then there are two generic scenarios. These are distinguished by the relative coexistence of the equilibrium undergoing the BEB, termed a *regular equilibrium*, and a *pseudo-equilibrium*: an equilibrium of the sliding dynamics. If these two equilibria do not coexist, we effectively have the ‘persistence’ of a single equilibrium. If the equilibria do coexist, then they collide and annihilate in a ‘nonsmooth-fold’. To determine which situation occurs for a given BEB, one can evaluate a certain inner product [8, 9].

To develop this further, let us recall what is known about BEBs in piecewise-smooth systems that are continuous but non-differentiable on discontinuity surfaces, in this context termed switching manifolds. For continuous systems, generic BEBs again conform to the two scenarios of persistence and a nonsmooth-fold, but here both equilibria are regular (one of each side of the switching manifold). Locally, the stability of these equilibria is determined by the eigenvalues of the Jacobian matrices of the two relevant smooth components of the system evaluated at the bifurcation. As was first shown for piecewise-smooth maps by Feigin [10] (for which the required calculations are almost identical), the BEB corresponds to persistence if the sum of the number of positive eigenvalues associated with each equilibrium is even, and is a nonsmooth-fold if this sum is odd [8].

Here we show that a similar result holds for Filippov systems, where now one equilibrium is a pseudo-equilibrium. The key step in our derivation is to use the matrix determinant lemma to connect the stability of the pseudo-equilibrium to the known inner product. An immediate consequence is that if both equilibria are stable, then neither has a positive eigenvalue and so the BEB corresponds to persistence.

In order to understand other invariant sets created in BEBs, it is in general not possible to employ dimension reduction techniques that are invaluable for high-dimensional smooth systems of ODEs. BEBs do not involve centre manifolds and so, as with maps [11], it appears that in n -dimensional systems BEBs can be inextricably n -dimensional [12].

BEBs are trivial in one dimension as equilibria are the only possible invariants. BEBs in two dimensions were studied in detail by Kuznetsov *et. al.* [13] but have only recently been completely classified. While it has long been known that there are eight topologically distinct cases for the generic local dynamics of a system at a BEB [14], some of these cases have multiple unfoldings and the realisation that there are exactly 12 topologically distinct BEBs in two dimensions was first made by Hogan *et. al.* [15].

To facilitate studies of BEBs in more than two dimensions, here we introduce an n -dimensional BEB normal form. Normal forms given previously typically use a real Jordan form or a symmetric matrix for the Jacobian matrix of the regular equilibrium [16, 17]. Here a companion matrix is used because, as with BEBs in continuous systems [8, 18], such matrices are well-suited for coordinate transformations that leave the discontinuity surface unchanged. As an added benefit, the Jacobian matrix of the pseudo-equilibrium is also a companion matrix. Below we show that a Filippov system with a non-degenerate BEB can be transformed to the normal form if and only if the Jacobian matrix of the regular equilibrium has no eigenvector tangent to the discontinuity surface.

The remainder of the paper is organised as follows. We first formulate BEBs in a general setting and clarify sliding motion, §2. We then compute equilibria, §3, and relate the relative coexistence of the equilibria to their associated eigenvalues, §4. Complete derivations are provided in §5 and consequences for codimension-two BEBs are discussed in §6. The normal form is introduced in §7, and its basic properties are discussed in §8. Section 9 relates the normal form in two dimensions to known results, and §10 provides a brief numerical exploration of the normal form in three dimensions. Here we discover a chaotic attractor (similar to Shilnikov chaos described by Glendinning [19]), multiple attractors, and the lack of an attractor in a case for which all associated eigenvalues have negative real part. Finally, conclusions are presented in §11.

Throughout this paper, e_1, \dots, e_n denote the standard basis vectors of \mathbb{R}^n , and $\mathbf{0} \in \mathbb{R}^n$ denotes the zero vector (or origin).

2 Preliminaries

We consider systems of the form

$$\dot{x} = \begin{cases} F^L(x; \mu), & x_1 < 0, \\ F^R(x; \mu), & x_1 > 0, \end{cases} \quad (1)$$

where F^L and F^R have continuous second derivatives. Here $x \in \mathbb{R}^n$ is the state variable and $\mu \in \mathbb{R}$ is a parameter. The discontinuity surface, call it Σ , is where the first component of x vanishes: $x_1 = 0$. For systems with discontinuity surfaces that take a more general form, say $H(x) = 0$, the idea is that one could apply a coordinate transformation to convert it to the form (1), at least locally.

Let

$$\chi(x; \mu) = F_1^L(x; \mu)F_1^R(x; \mu), \quad (2)$$

be the product of the first components of F^L and F^R . Subsets of Σ for which $\chi > 0$ are *crossing regions* (in Fig. 1-A we have $F_1^L > 0$ and $F_1^R > 0$). Subsets of Σ for which $\chi < 0$ are *sliding regions*. A sliding region is *attracting* if $F_1^L > 0$ and $F_1^R < 0$ (as in Fig. 1-B), and *repelling* if $F_1^L < 0$ and $F_1^R > 0$.

Dynamics on a sliding region are governed by $\dot{x} = F^S(x; \mu)$ where

$$F^S = \frac{F_1^L F^R - F_1^R F^L}{F_1^L - F_1^R}, \quad (3)$$

is the unique convex combination of F^L and F^R for which $F_1^S = 0$ [8, 14].

Now suppose F^L has an equilibrium at $x = \mathbf{0}$ when $\mu = 0$, as illustrated in Fig. 2. Then

$$F^L(x; \mu) = Ax + b\mu + \mathcal{O}(2), \quad (4)$$

for some $n \times n$ matrix A and $b \in \mathbb{R}^n$, and we write $\mathcal{O}(k)$ for terms that are order k or greater in x and μ . Notice that A is the Jacobian matrix $DF^L(\mathbf{0}; 0)$. Also

$$F^R(x; \mu) = c + \mathcal{O}(1), \quad (5)$$

for some $c \in \mathbb{R}^n$, and so our system has the form

$$\dot{x} = \begin{cases} Ax + b\mu + \mathcal{O}(2), & x_1 < 0, \\ c + \mathcal{O}(1), & x_1 > 0. \end{cases} \quad (6)$$

Locally, orbits in $x_1 > 0$ approach Σ (as time increases) if $c_1 < 0$, and head away from Σ if $c_1 > 0$. By substituting the above expressions for F^L and F^R into (3), we obtain

$$F^S(x; \mu) = \left(I - \frac{ce_1^T}{c_1} \right) (Ax + b\mu) + \mathcal{O}(2), \quad (7)$$

assuming $c_1 \neq 0$.

3 Equilibria

A *regular equilibrium* of (1) is a point $x \in \mathbb{R}^n$ for which $F^L(x; \mu) = \mathbf{0}$ or $F^R(x; \mu) = \mathbf{0}$. For the system (6), $F^R(x; \mu) = \mathbf{0}$ has no local solution if $c \neq \mathbf{0}$. Solving $F^L(x; \mu) = \mathbf{0}$ yields

$$x^L(\mu) = -A^{-1}b\mu + \mathcal{O}(\mu^2), \quad (8)$$

assuming $\det(A) \neq 0$, and so we have the following result.

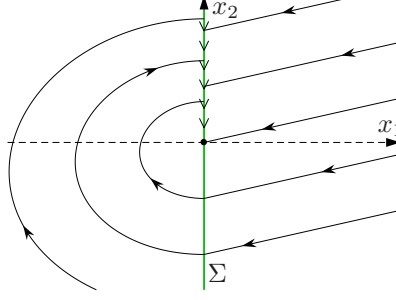


Figure 2: A typical phase portrait of (6) with $\mu = 0$ (i.e. at the BEB).

Lemma 1. *If $\det(A) \neq 0$ and $c \neq \mathbf{0}$, then, in a neighbourhood of $(x; \mu) = (\mathbf{0}, 0)$, the system (6) has a unique regular equilibrium $x^L(\mu)$ given by (8).*

Since F^L only applies to points with $x_1 < 0$, we say that x^L is *admissible* if $x_1^L < 0$, and *virtual* if $x_1^L > 0$.

A *pseudo-equilibrium* of (1) is a point $x \in \Sigma$ for which $F^S(x; \mu) = \mathbf{0}$. To calculate pseudo-equilibria of (6), first observe that the form (7) hides the fact that sliding dynamics is $(n - 1)$ -dimensional. In (7) we are assuming $x_1 = 0$; also $\dot{x}_1 = 0$. For this reason, we let \tilde{M} denote the lower-right $(n - 1) \times (n - 1)$ block of

$$M = DF^S(\mathbf{0}; 0) = \left(I - \frac{ce_1^T}{c_1} \right) A. \quad (9)$$

The matrix \tilde{M} is the Jacobian of the sliding dynamics evaluated at $(x; \mu) = (\mathbf{0}, 0)$, and so we have the following result.

Lemma 2. *If $\det(\tilde{M}) \neq 0$ and $c_1 \neq 0$, then, in a neighbourhood of $(x; \mu) = (\mathbf{0}, 0)$, the system (6) has a unique pseudo-equilibrium $x^S(\mu)$.*

Notice $F^S(\mathbf{0}; 0) = \mathbf{0}$, thus, by uniqueness, $x^S(0) = \mathbf{0}$. Since F^S only applies to points in sliding regions of Σ , we say that x^S is *admissible* if $\chi(x^S(\mu); \mu) < 0$, and *virtual* if $\chi(x^S(\mu); \mu) > 0$.

Now let us think about how the admissibility of x^L and x^S change as the value of μ changes sign. Since $x^L(0) = x^S(0) = \mathbf{0}$, we can write

$$x_1^L(\mu) = \alpha_L \mu + \mathcal{O}(\mu^2), \quad (10)$$

$$\chi(x^S(\mu); \mu) = \alpha_S \mu + \mathcal{O}(\mu^2), \quad (11)$$

for some $\alpha_L, \alpha_S \in \mathbb{R}$. Then x^L is admissible if $\alpha_L \mu < 0$, and x^S is admissible if $\alpha_S \mu < 0$. If x^L and x^S are admissible for different signs of μ , the BEB is referred to as *persistence*, Fig. 3-A. If x^L and x^S are admissible for the same sign of μ , the BEB is referred to as a *nonsmooth-fold*, Fig. 3-B. Immediately we have the following result.

Lemma 3. *Suppose $\det(A) \neq 0$, $\det(\tilde{M}) \neq 0$, and $c_1 \neq 0$. Then the BEB at $\mu = 0$ corresponds to persistence if $\alpha_L \alpha_S < 0$, and to a nonsmooth-fold if $\alpha_L \alpha_S > 0$.*

Computations of α_L and α_S form the subject of the next two sections.

4 Feigin analysis

In a key 1978 paper [10], Feigin showed that for border-collision bifurcations of piecewise-smooth continuous maps, the existence and relative coexistence of fixed points and period-two solutions can be determined, in a simple way, from the eigenvalues of the two corresponding Jacobian matrices. For BEBs of piecewise-smooth continuous ODEs, the computations are almost identical [8]. The following result (proved in §5) shows how this ‘Feigin analysis’ extends to BEBs of (6). We assume $\alpha_L \neq 0$ to ensure that μ unfolds the bifurcation in a generic fashion (see also the comments at the start of §5). For any $a \in \mathbb{R}$, we write

$$\text{sgn}(a) = \begin{cases} -1, & a < 0, \\ 0, & a = 0, \\ 1, & a > 0. \end{cases} \quad (12)$$

Theorem 4. *Suppose $\det(A) \neq 0$, $\det(\tilde{M}) \neq 0$, $c_1 \neq 0$, and $\alpha_L \neq 0$. Then*

$$\text{sgn}(\alpha_L \alpha_S) = (-1)^{N_L + N_S} \text{sgn}(c_1), \quad (13)$$

where N_L is the number of real positive eigenvalues of A , and N_S is the number of real positive eigenvalues of \tilde{M} .

Theorem 4 is practical in the sense that it shows how the BEB can be classified from a simple calculation. The matrices A and \tilde{M} govern the stability of x^L and x^S and their local dynamics. This is because the Jacobian matrix DF^L evaluated at $x^L(\mu)$ is equal to $A + \mathcal{O}(\mu)$. Thus, if A has no eigenvalues with zero real part, then, for all sufficiently small values of μ for which $x^L(\mu)$ is admissible, the dimension of the unstable manifold of $x^L(\mu)$ is equal to the number of eigenvalues of A (counting algebraic multiplicity) with positive real part. If we let D_L denote this dimension, then

$$(-1)^{D_L} = (-1)^{N_L}, \quad (14)$$

because complex eigenvalues of A appear in complex conjugate pairs.

More care is required to describe the stability of the pseudo-equilibrium x^S in the same manner. In the context of the $(n-1)$ -dimensional sliding dynamics, if \tilde{M} has no eigenvalues with zero real part, then the dimension of the unstable manifold of $x^S(\mu)$, call it \tilde{D}_S , is equal

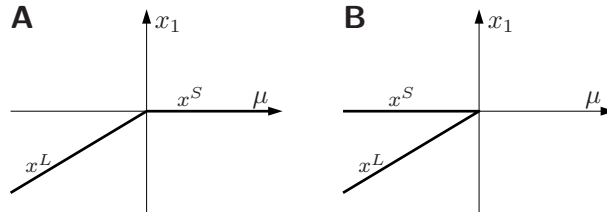


Figure 3: Typical bifurcation diagrams of (6) showing persistence (panel A) and a nonsmooth-fold (panel B).

to the number of eigenvalues of \tilde{M} (counting algebraic multiplicity) with positive real part, and, as above, $(-1)^{\tilde{D}_S} = (-1)^{N_S}$. For the full system (6), we look at the type of sliding region to which x^S belongs. If $c_1 < 0$, then the sliding region is attracting, and so the dimension of the unstable manifold of $x^S(\mu)$, call it D_S , is equal to \tilde{D}_S . If instead $c_1 > 0$, then the sliding region is repelling, and so $D_S = \tilde{D}_S + 1$. In summary,

$$(-1)^{D_S} = \begin{cases} (-1)^{N_S}, & c_1 < 0, \\ (-1)^{N_S+1}, & c_1 > 0. \end{cases} \quad (15)$$

By then combining (13)–(15) we obtain

$$\text{sgn}(\alpha_L \alpha_S) = (-1)^{D_L + D_S + 1}, \quad (16)$$

which connects the classification of the BEB to the dimensions of the unstable manifolds of the equilibria. In practice these dimensions may be known from numerical simulations. In particular, if both x^L and x^S are stable, then $D_L = D_S = 0$, thus $\alpha_L \alpha_S < 0$, and hence the BEB corresponds to persistence by Lemma 3.

5 Proof of Theorem 4

The *adjugate* of A , denoted $\text{adj}(A)$, is the transpose of the cofactor matrix of A . In particular, if $\det(A) \neq 0$, then $\text{adj}(A) = \det(A)A^{-1}$. As with continuous piecewise-smooth systems [20], we let

$$\varrho^\top = e_1^\top \text{adj}(A). \quad (17)$$

Then, by (8) and (10),

$$\alpha_L = -\frac{\varrho^\top b}{\det(A)}. \quad (18)$$

Recall, we require $\det(A) \neq 0$ so that x^L is well-defined and unique. From (18) we see that $\varrho^\top b \neq 0$ is needed to ensure that $x^L(\mu)$ moves away from Σ as the value of μ is varied from 0 at an asymptotically linear rate. That is, $\varrho^\top b \neq 0$ is the *transversality condition* for the BEB.

As mentioned in §1, the distinction between persistence and a nonsmooth-fold has previously been equated to the sign of a certain inner product [8, 9]. For our system (6), this inner product is $\varrho^\top c$ and appears in the following result.

Lemma 5. *Suppose $\det(A) \neq 0$, $\det(\tilde{M}) \neq 0$, $c_1 \neq 0$, and $\varrho^\top c \neq 0$. Then*

$$F_1^L(x^S(\mu); \mu) = \frac{\varrho^\top b c_1}{\varrho^\top c} \mu + \mathcal{O}(\mu^2). \quad (19)$$

The following proof of Lemma 5 closely follows that of di Bernardo *et. al.* [8].

Proof. The pseudo-equilibrium satisfies $F^S(x^S(\mu); \mu) = \mathbf{0}$. By (7) we can rewrite F^S as

$$F^S(x; \mu) = F^L(x; \mu) - \frac{F_1^L(x; \mu)}{c_1} c + \mathcal{O}(2). \quad (20)$$

By multiplying this on the left by ϱ^\top and substituting $x = x^S(\mu)$ we obtain

$$0 = \varrho^\top F^L(x^S(\mu); \mu) - \frac{F_1^L(x^S(\mu); \mu) \varrho^\top c}{c_1} + \mathcal{O}(\mu^2). \quad (21)$$

The first term in (21) simplifies to $\varrho^\top b \mu$ (because $x_1^S(\mu) = 0$) and so the desired expression (19) results from a simple rearrangement of (21). \square

The next result, which to the best of the author's knowledge is new, shows how the inner product $\varrho^\top c$ is related to the Jacobian matrix \tilde{M} .

Lemma 6. *Suppose $\det(A) \neq 0$ and $c_1 \neq 0$. Then*

$$\det(\tilde{M}) = \frac{\varrho^\top c}{c_1}. \quad (22)$$

Proof. Since the first row of M is $\mathbf{0}^\top$, the characteristic polynomials of M and \tilde{M} are related by

$$\det(\lambda I - M) = \lambda \det(\lambda I - \tilde{M}). \quad (23)$$

To evaluate $\det(\lambda I - M)$, we use the matrix determinant lemma: $\det(X + vu^\top) = \det(X)(1 + u^\top X^{-1}v)$, for any non-singular $n \times n$ matrix X and $u, v \in \mathbb{R}^n$. From (9) we obtain

$$\det(\lambda I - M) = \det(\lambda I - A) \left(1 + \frac{e_1^\top A(\lambda I - A)^{-1} c}{c_1} \right).$$

By then substituting $(\lambda I - A)^{-1} = -A^{-1} - A^{-2}\lambda + \mathcal{O}(\lambda^2)$, we produce

$$\det(\lambda I - M) = -\frac{\det(-A)}{c_1} e_1^\top A^{-1} c \lambda + \mathcal{O}(\lambda^2).$$

By (17) this reduces to

$$\det(\lambda I - M) = \frac{(-1)^{n+1} \varrho^\top c}{c_1} \lambda + \mathcal{O}(\lambda^2).$$

Thus by (23) we have $\det(-\tilde{M}) = \frac{(-1)^{n+1} \varrho^\top c}{c_1}$, and hence (22), as required. \square

By combining (19), (22), and $F_1^R(x^S(\mu); \mu) = c_1 + \mathcal{O}(\mu)$, we arrive at

$$\alpha_S = \frac{\varrho^\top b c_1}{\det(\tilde{M})}. \quad (24)$$

To complete the proof of Theorem 4, we combine (18) and (24) to obtain

$$\text{sgn}(\alpha_L \alpha_S) = -\text{sgn}(\det(A) \det(\tilde{M}) c_1). \quad (25)$$

Notice $(-1)^{N_L} = \text{sgn}(\det(-A))$, and $(-1)^{N_S} = \text{sgn}(\det(-\tilde{M}))$. Also $\det(A) = (-1)^n \det(-A)$, and $\det(\tilde{M}) = (-1)^{n+1} \det(-\tilde{M})$. Therefore (25) is equivalent to the given formula (13).

6 A remark on codimension-two BEBs

The above results add insight into some codimension-two BEBs. Suppose the two-dimensional parameter space of a Filippov system has a curve of BEBs. Further suppose that at a point on this curve the BEBs change from persistence to a nonsmooth-fold. That is, one of α_L and α_S changes sign. The case that α_L changes sign was unfolded for a simple system by di Bernardo *et. al.* [21]; the case that α_S changes sign was unfolded in a general setting by Della Rossa and Dercole [22]. In both cases a curve of saddle-node bifurcations emanates from the codimension-two point with a quadratic tangency. This is illustrated in Fig. 4. The same unfolding occurs for the analogous scenario in continuous piecewise-smooth systems [23].

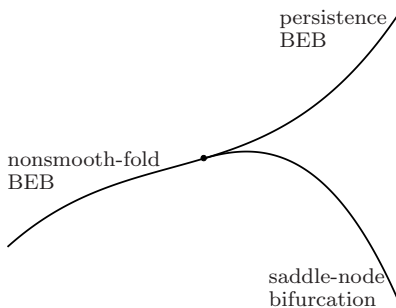


Figure 4: A sketch of a typical two-parameter bifurcation diagram of a Filippov system about a codimension-two point where a curve of BEBs changes from persistence to nonsmooth-fold type.

These unfoldings assume that in a neighbourhood of the codimension-two point the transversality condition of the BEBs is satisfied (i.e. $\varrho^T b \neq 0$). It is also assumed that, locally, the system without a regular equilibrium has no tangency with the discontinuity surface (i.e. $c_1 \neq 0$). Then by (18) and (24), α_L and α_S must change sign, not by becoming zero, but rather by going ‘through infinity’ by either $\det(A) = 0$ or $\det(\tilde{M}) = 0$. This tells us that at the codimension-two point one of the equilibria has a zero eigenvalue, and this provides an explanation for the presence of saddle-node bifurcations.

7 A normal form

Here we introduce the normal form

$$\dot{x} = \begin{cases} Cx + e_n \mu, & x_1 < 0, \\ d, & x_1 > 0, \end{cases} \quad (26)$$

where C is the companion matrix

$$C = \begin{bmatrix} -a_1 & 1 & & \\ -a_2 & & \ddots & \\ \vdots & & & 1 \\ -a_n & & & \end{bmatrix}, \quad (27)$$

and $d \in \mathbb{R}^n$ with $d_1 = \pm 1$. The $a_i \in \mathbb{R}$ are the coefficients of the characteristic polynomial of C :

$$\det(\lambda I - C) = \lambda^n + a_1 \lambda^{n-1} + \cdots + a_{n-1} \lambda + a_n. \quad (28)$$

The following theorem justifies our interpretation of (26) as a ‘normal form’ for BEBs by providing a coordinate transformation from a system in the general form (6) to (26). Since (6) is piecewise-smooth, it may tempting to apply different coordinate transformations to the two pieces of (6). However, this may alter the sliding dynamics in a fundamental way. Indeed, as we will see, a single coordinate transformation is sufficient. In the following result, J denotes the companion matrix (27) for which $a_i = 0$ for all i .

Theorem 7. *Consider a system of the form (6) with $c_1 \neq 0$. Let $a_1, \dots, a_n \in \mathbb{R}$ be the coefficients of the characteristic polynomial of A (matching (28)). Let*

$$\begin{aligned} \Psi &= \begin{bmatrix} 1 & & & \\ a_1 & 1 & & \\ \vdots & \ddots & \ddots & \\ a_{n-1} & \cdots & a_1 & 1 \end{bmatrix}, \\ \Phi &= \begin{bmatrix} e_1^\top \\ e_1^\top A \\ \vdots \\ e_1^\top A^{n-1} \end{bmatrix}, \end{aligned} \quad (29)$$

and

$$\begin{aligned} Q &= \Psi \Phi, \\ r &= J^\top Q b, \\ s &= e_n^\top Q b. \end{aligned} \quad (30)$$

If $\det(\Phi) \neq 0$ and $s \neq 0$, then under the coordinate transformation

$$\begin{aligned} x &\mapsto Qx + r\mu, \\ \mu &\mapsto s\mu, \end{aligned} \quad (31)$$

the system (6) becomes

$$\dot{x} = \begin{cases} Cx + e_n \mu + \mathcal{O}(2), & x_1 < 0, \\ d + \mathcal{O}(1), & x_1 > 0, \end{cases} \quad (32)$$

where C is given by (27) and $d = Qc$. The additional transformation, $x \mapsto \frac{1}{|d_1|}x$ and $\mu \mapsto \frac{1}{|d_1|}\mu$, scales the first element of d to ± 1 .

The normal form (26) results from removing higher order terms from (32). We do not provide a proof of Theorem 7 as it is a trivial generalisation of that for continuous piecewise-smooth systems [24]. The use of companion matrices stems from control theory [8]. Indeed,

Φ is called an *observability matrix* and, as in the continuous setting, we say that the system (6) is ‘observable’ if $\det(\Phi) \neq 0$.

It is typical for a given system (6) to be observable. Indeed the ‘Popov-Belevitch-Hautus observability test’ [25] (a control theory result) tells us that (6) is observable if and only if A does not have an eigenvector orthogonal to e_1 [26]. For the unfolding of a codimension-two BEB at which A has an eigenvector orthogonal to e_1 , refer to Section 8 of Guardia *et. al.* [27].

Note that $e_1^\top Q = e_1^\top$ and $r_1 = 0$, due to the way Ψ and Φ are defined. Hence the coordinate transformation (31) leaves x_1 unchanged, and $d_1 = c_1$. Thus the assumption $c_1 \neq 0$ ensures that the additional transformation in Theorem 7 is well-defined.

8 Properties of the normal form

Here we study (26) (where $d_1 = \pm 1$). If $a_n \neq 0$ (equivalently, if $\det(C) \neq 0$), then (26) has the unique regular equilibrium $x^L(\mu) = -e_1^\top C^{-1} e_n \mu$. In particular, $x_1^L(\mu) = \frac{1}{a_n} \mu$, thus x^L moves linearly away from the discontinuity surface Σ as μ is varied from 0. That is, the transversality condition is automatically satisfied in the normal form. This tells us that if the coordinate transformation from (6) to (26) can be achieved, then the transversality condition needs to be satisfied in (6) (this condition is $\varrho^\top b \neq 0$). Indeed, via direct calculations and the Cayley Hamilton theorem, it can be shown that $s = (-1)^{n+1} \varrho^\top b$, and $s \neq 0$ is required in Theorem 7.

Next we study the sliding dynamics of (26). For the $x_1 < 0$ component of (26), with $x_1 = 0$ we have $\dot{x}_1 = x_2$. Thus if $d_1 = -1$, then $x_2 > 0$ is an attracting sliding region and $x_2 < 0$ is a crossing region. If instead $d_1 = 1$, then $x_2 > 0$ is a crossing region and $x_2 < 0$ is a repelling sliding region.

Sliding dynamics are governed by (3) applied to (26). If we are only interested in the paths that orbits take, not evolution times, we can scale time in a spatially dependent way so that the denominator of (3) changes from $F_1^L - F_1^R$ to $-F_1^R$. This is a common strategy for dealing with sliding motion [14], and particularly beneficial here as the resulting scaled sliding vector field is linear, specifically:

$$\begin{bmatrix} \dot{x}_2 \\ \vdots \\ \dot{x}_n \end{bmatrix} = \tilde{M} \begin{bmatrix} x_2 \\ \vdots \\ x_n \end{bmatrix} + \begin{bmatrix} 0 \\ \vdots \\ 0 \\ \mu \end{bmatrix}, \quad (33)$$

where

$$\tilde{M} = \begin{bmatrix} -\frac{d_2}{d_1} & 1 & & \\ -\frac{d_3}{d_1} & & \ddots & \\ \vdots & & & \\ -\frac{d_n}{d_1} & & & 1 \end{bmatrix}. \quad (34)$$

Notice that (33) has the same form as the $x_1 < 0$ component of (26), except it is of one less dimension. In particular, the coefficients of the characteristic polynomial of \tilde{M} are $\frac{d_2}{d_1}, \dots, \frac{d_n}{d_1}$.

Sliding motion ceases at $x_2 = 0$. Here (33) has $\dot{x}_2 = x_3$ (assuming $n \geq 3$). Thus the direction of sliding motion at $x_2 = 0$ is governed by the sign of x_3 . In particular, if $d_1 = -1$ then sliding orbits can only escape the attracting sliding region $x_2 > 0$ at points on $x_2 = 0$ with $x_3 < 0$.

Since (26) and (33) have no quadratic or higher order terms, the structure of the dynamics is independent of the magnitude of μ . All bounded invariant sets collapse linearly to the origin as $\mu \rightarrow 0$, and to understand the dynamics it suffices to consider $\mu \in \{-1, 0, 1\}$.

9 BEBs in two dimensions

Here we consider (26) in two dimensions with $d_1 = -1$ (the case $d_1 = 1$ can be understood via a reversal of time). We write

$$C = \begin{bmatrix} \tau_L & 1 \\ -\delta_L & 0 \end{bmatrix},$$

so that τ_L and δ_L are the trace and determinant of C . By (34), we have $\tilde{M} = d_2$ (a scalar). In summary, (26) has three parameters $(\tau_L, \delta_L, d_2 \in \mathbb{R})$ in addition to the BEB parameter $\mu \in \mathbb{R}$. The scaled sliding vector field is

$$\dot{x}_2 = d_2 x_2 + \mu.$$

With $\mu = 0$, the origin is a boundary equilibrium. In two dimensions there are eight topologically distinct non-degenerate scenarios for the dynamics local to a boundary equilibrium [14]. These are nicely characterised by the parameters in our normal form. The regular equilibrium x^L is (i) a saddle if $\delta_L < 0$, (ii) an attracting node if $\tau_L < 0$ and $0 < \delta_L < \frac{\tau_L^2}{4}$, (iii) a repelling node if $\tau_L > 0$ and $0 < \delta_L < \frac{\tau_L^2}{4}$, and (iv) a focus if $\delta_L > \frac{\tau_L^2}{4}$. Sliding motion is directed towards the origin if $d_2 < 0$, and away from the origin if $d_2 > 0$. These two sets of criteria are independent and by combining them we obtain the eight generic scenarios illustrated in Fig. 5.

These eight boundary equilibria can be unfolded by varying the value of μ in the normal form. Some of these have multiple unfoldings. For instance the lower-left boundary equilibrium of Fig. 5 has two generic unfoldings: an attracting limit cycle exists for $\mu < 0$ if the focus is repelling; no limit cycle exists if the focus is attracting. The upper-left boundary equilibrium has two unfoldings, the lower-right boundary equilibrium has three unfoldings, and the remainder have one unfolding (see [17, 15] for details). Thus there are 12 generic BEBs in two dimensions.

10 BEBs in three dimensions

Here we consider (26) in three dimensions with $d_1 = -1$. We write

$$C = \begin{bmatrix} \tau_L & 1 & 0 \\ -\sigma_L & 0 & 1 \\ \delta_L & 0 & 0 \end{bmatrix},$$

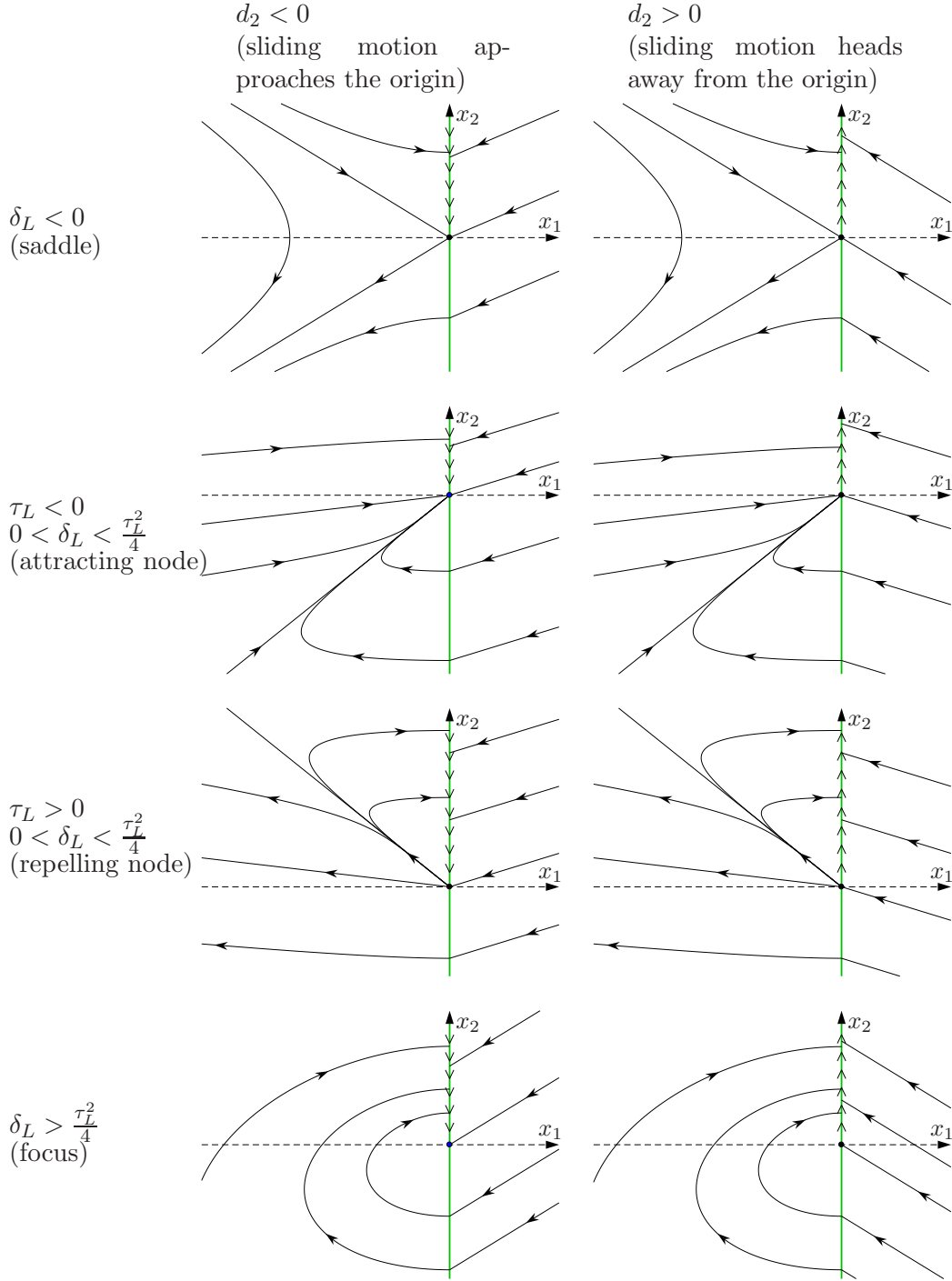


Figure 5: Filippov's eight scenarios for the dynamics local to a non-degenerate boundary equilibrium in two dimensions as exemplified by the normal form (26) with $d_1 = -1$.

so that τ_L , σ_L , and δ_L are the trace, second trace, and determinant of C (see Appendix C of Simpson [28]). We write

$$d = \begin{bmatrix} -1 \\ \tau_S \\ -\delta_S \end{bmatrix},$$

so that τ_S and δ_S are the trace and determinant of

$$\tilde{M} = \begin{bmatrix} \tau_S & 1 \\ -\delta_S & 0 \end{bmatrix}.$$

Thus there are five parameters ($\tau_L, \sigma_L, \delta_L, \tau_S, \delta_S \in \mathbb{R}$) in addition to μ .

Glendinning [19] identified a Shilnikov homoclinic orbit in a three-dimensional system of the form (6). This shows that the dynamical properties associated with Shilnikov homoclinic orbits, such as chaos, can be generated in BEBs in three dimensions.

As an example, we use the parameter values

$$\begin{aligned} \tau_L &= -0.5, \\ \sigma_L &= 4, \\ \delta_L &= 2, \end{aligned} \tag{35}$$

so that the regular equilibrium is a saddle-focus (necessary for a Shilnikov homoclinic orbit). We also fix $\delta_S = 1$ and consider various values of τ_S .

Fig. 6 shows a phase portrait of (26) with $\tau_S = 0.275$ and $\mu = 1$ (with instead $\mu = -1$ the system does not appear to have a bounded attractor). Here both x^L and x^S are admissible and unstable (the BEB is of nonsmooth-fold type; in Theorem 4 we have $N_L = 1$, $N_S = 0$, and $c_1 < 0$). Since the system is linear in $x_1 < 0$, the stable and unstable manifolds of x^L are linear as they emanate from x^L (as shown in Fig. 6) only becoming curved once they intersect Σ . There is both an attracting limit cycle and an apparently chaotic attractor. Thus two attractors are created in the BEB at $\mu = 0$. The creation of multiple attractors in a BEB (for both Filippov systems and continuous systems) does not appear to have been reported previously.

Next we construct a Poincaré map to better understand these attractors. As discussed in §8, sliding motion on Σ turns into regular motion in $x_1 < 0$ along the line $x_1 = x_2 = 0$ with $x_3 < 0$. We let Γ denote this half-line and P denote the Poincaré map on Γ . That is, for any $x_3 < 0$, we let $P(x_3)$ be such that the forward orbit of $(0, 0, x_3)$ next intersects Γ at $(0, 0, P(x_3))$, and let $P(x_3)$ be undefined if the orbit does not return to Γ . The map P captures all invariant sets of (26) that involve both sliding motion and regular motion. The only other bounded invariant sets of (26) are the equilibria, x^L and x^S , because the sliding and regular dynamics are governed by linear systems.

Fig. 7 shows P using the same parameter values as Fig. 6. The cobweb diagram indicates the apparently chaotic attractor. The stable fixed point of P (shaded blue) corresponds to the attracting limit cycle. The two unstable fixed points of P (shaded red) correspond to unstable limit cycles. The map P has oscillations accumulating at $x_3 \approx -2.21$ for which the forward orbit of $(0, 0, x_3)$ converges to x^L , for details see Glendinning [19].

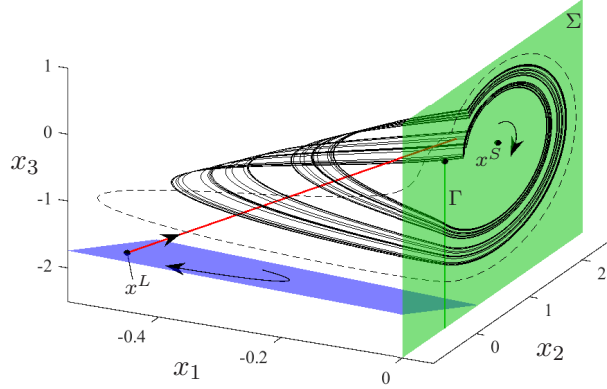


Figure 6: A phase portrait of the normal form (26) in three dimensions. Specifically the parameter values are (35), $\tau_S = 0.275$, $\delta_S = 1$, and $\mu = 1$. A stable limit cycle is shown with a dashed curve; an apparently chaotic attractor is shown with a solid curve. The regular equilibrium x^L is a saddle-focus; the pseudo-equilibrium x^S is an unstable focus.

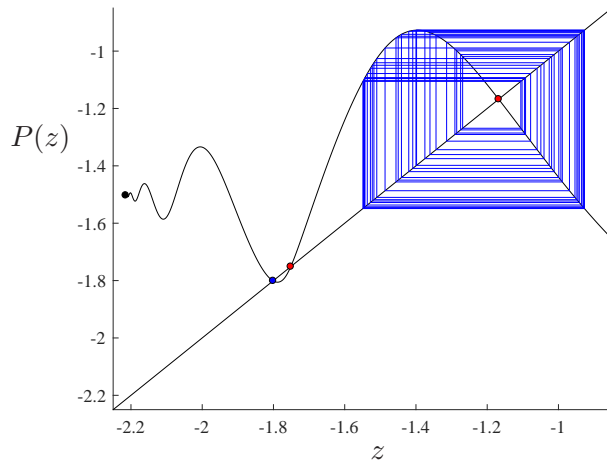


Figure 7: The Poincaré map P for the parameter values of Fig. 6.

Fig. 8 shows a bifurcation diagram of (26) produced by varying the value of τ_S . More specifically, Fig. 8 indicates the long-term behaviour of P with the initial value $x_3 = -1$. By using this particular initial value, we observe bifurcations leading to the apparently chaotic attractor of Fig. 6. In particular we see period-doubling cascades and windows of periodicity (typical for smooth non-invertible one-dimensional maps) as well as adding-sliding bifurcations [8] at $\tau_S \approx 0.142$ and $\tau_S \approx 0.163$ where the attractor includes the value $x_3 = 0$.

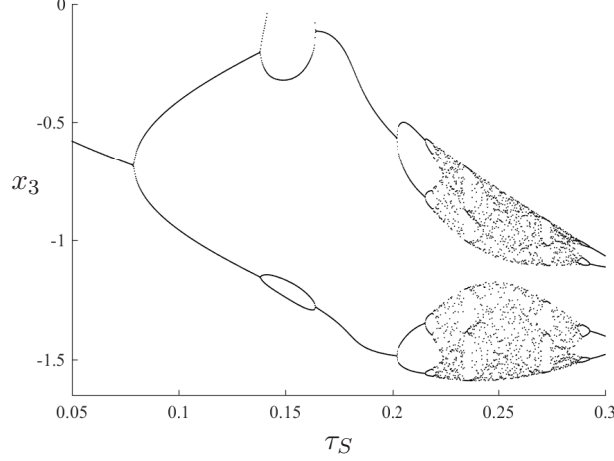


Figure 8: A bifurcation diagram of the normal form (26) in three dimensions using the parameter values (35), $\delta_S = 1$, and $\mu = 1$. The vertical axis represents the x_3 -value on Γ (where $x_1 = x_2 = 0$).

Finally we consider the parameter values

$$\begin{aligned}
 \tau_L &= -0.3, \\
 \sigma_L &= 0.4, \\
 \delta_L &= -0.1, \\
 \tau_S &= -0.2, \\
 \delta_S &= 1.
 \end{aligned} \tag{36}$$

For these values all eigenvalues of C and \tilde{M} have negative real part. Thus, when admissible, the equilibria x^L and x^S are asymptotically stable. Yet, as shown in Fig. 9, with $\mu = 0$ the origin is unstable. This is because the system has an invariant cone involving a sector of Σ over which orbits head outwards, and this dominates the inwards motion in $x_1 < 0$ to create a net outwards motion. This counter-intuitive result is not possible in less than three dimensions and is well-known for continuous systems [29].

11 Discussion

The n -dimensional normal form (26) has $2n - 1$ parameters (not counting the BEB parameter $\mu \in \mathbb{R}$, or $d_1 = \pm 1$). The parameters are $a_1, \dots, a_n \in \mathbb{R}$, which appear in the companion matrix C , and $d_2, \dots, d_n \in \mathbb{R}$, which appear in the vector d . For a given BEB in a system of the form (6), the values of these parameters can be determined by explicitly applying the coordinate transformation of Theorem 7, or, more simply, they can be determined from the eigenvalues of $A = DF^L(\mathbf{0}; 0)$ and $M = DF^S(\mathbf{0}; 0)$, as follows. First set $d_1 = \text{sgn}(c_1)$. The eigenvalues of A uniquely determine a_1, \dots, a_n because these numbers are the coefficients of the characteristic polynomial of A (we know that A and C are similar). The eigenvalues of

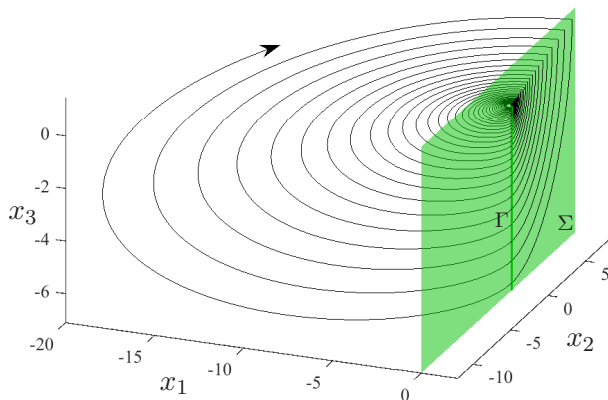


Figure 9: A phase portrait of (26) in three dimensions with (36) and $\mu = 0$.

M uniquely determine d_2, \dots, d_n in a similar fashion. Specifically, M has a zero eigenvalue, and the remaining $n - 1$ eigenvalues are those of \tilde{M} , whose characteristic polynomial has coefficients $\frac{d_2}{d_1}, \dots, \frac{d_n}{d_1}$, see (34). Moreover, we conclude that the eigenvalues of A and M fully determine all structurally stable features of the dynamics local to the BEB, assuming non-degeneracy conditions are satisfied.

The normal form is intended to provide a foundation by which BEBs can be analysed in systems of any number of dimensions. Generic BEBs in two dimensions have been completely classified [15]. This paper reveals new complexities for BEBs in three dimensions, such as the creation of multiple attractors. The results of §10 provide numerical evidence for the creation of a chaotic attractor in a BEB, but the given example has no equilibrium on the other side of the BEB. It remains to be determined if a stable equilibrium can bifurcate to a chaotic attractor in a BEB of a Filippov system (this has been found numerically in continuous systems [30]).

In §10 the three-dimensional dynamics was captured with a Poincaré map P . For smooth three-dimensional systems of ODEs, Poincaré maps are two-dimensional. Here P is one-dimensional because orbits become constrained to the codimension-one discontinuity surface Σ . Yet, as in Fig. 7, P may be non-invertible. This is because the contraction of orbits onto Σ is a non-invertible process, and permits the dynamics to be chaotic. If we were to smooth the system by mollifying the switching condition, the dynamics would be captured by a two-dimensional Poincaré map. This map would be invertible but well-approximated by the one-dimensional non-invertible map P . The approximation of three-dimensional dynamics with a one-dimensional map occurs also for the dynamics associated with a Shilnikov homoclinic orbit [31] and an orbit homoclinic to a limit cycle [32], for example.

References

- [1] B. Blazejczyk-Okolewska, K. Czołczynski, T. Kapitaniak, and J. Wojewoda. *Chaotic Mechanics in Systems with Impacts and Friction*. World Scientific, Singapore, 1999.
- [2] M. Johansson. *Piecewise Linear Control Systems.*, volume 284 of *Lecture Notes in Control and Information Sciences*. Springer-Verlag, New York, 2003.
- [3] F. Dercole, A. Gagnani, and S. Rinaldi. Bifurcation analysis of piecewise smooth ecological models. *Theor. Popul. Biol.*, 72:197–213, 2007.
- [4] F. Dercole, F. Della Rossa, and Yu.A. Colombo, A. Kuznetsov. Two degenerate boundary equilibrium bifurcations in planar Filippov systems. *SIAM J. Appl. Dyn. Syst.*, 10(4):1525–1553, 2011.
- [5] V. Křivan. On the Gause predator-prey model with a refuge: A fresh look at the history. *J. Theoret. Biol.*, 274:67–73, 2011.
- [6] S. Tang, J. Liang, Y. Xiao, and R.A. Cheke. Sliding bifurcations of Filippov two stage pest control models with economic thresholds. *SIAM J. Appl. Math.*, 72(4):1061–1080, 2012.
- [7] J. Walsh, E. Widiasih, J. Hahn, and R. McGehee. Periodic orbits for a discontinuous vector field arising from a conceptual model of glacial cycles. *Nonlinearity*, 29(6):1843–1864, 2016.
- [8] M. di Bernardo, C.J. Budd, A.R. Champneys, and P. Kowalczyk. *Piecewise-smooth Dynamical Systems. Theory and Applications*. Springer-Verlag, New York, 2008.
- [9] M. di Bernardo, D.J. Pagano, and E. Ponce. Nonhyperbolic boundary equilibrium bifurcations in planar Filippov systems: A case study approach. *Int. J. Bifurcation Chaos*, 18(5):1377–1392, 2008.
- [10] M.I. Feigin. On the structure of C -bifurcation boundaries of piecewise-continuous systems. *J. Appl. Math. Mech.*, 42(5):885–895, 1978. Translation of *Prikl. Mat. Mekh.*, 42(5):820–829, 1978.
- [11] P. Glendinning and M.R. Jeffrey. Grazing-sliding bifurcations, border collision maps and the curse of dimensionality for piecewise smooth bifurcation theory. *Nonlinearity*, 28:263–283, 2015.
- [12] P. Glendinning. Less is more I: A pessimistic view of piecewise smooth bifurcation theory. In A. Colombo, M. Jeffrey, J. Lázaro, and J. Olm, editors, *Extended Abstracts Spring 2016*, volume 8 of *Trends in Mathematics*, pages 71–75. Birkhäuser, Cham, 2017.
- [13] Yu.A. Kuznetsov, S. Rinaldi, and A. Gagnani. One-parameter bifurcations in planar Filippov systems. *Int. J. Bifurcation Chaos*, 13(8):2157–2188, 2003.

- [14] A.F. Filippov. *Differential Equations with Discontinuous Righthand Sides*. Kluwer Academic Publishers., Norwell, 1988.
- [15] S.J. Hogan, M.E. Homer, M.R. Jeffrey, and R. Szalai. Piecewise smooth dynamical systems theory: the case of the missing boundary equilibrium bifurcations. *J. Nonlin. Sci.*, 26:1161–1173, 2016.
- [16] T. de Carvalho and D.J. Tonon. Normal forms for codimension one planar piecewise smooth vector fields. *Int. J. Bifurcation Chaos*, 24(7):1450090, 2014.
- [17] P. Glendinning. Classification of boundary equilibrium bifurcations in planar Filippov systems. *Chaos*, 26:013108, 2016.
- [18] V. Carmona, E. Freire, E. Ponce, and F. Torres. On simplifying and classifying piecewise-linear systems. *IEEE Trans. Circuits Systems I Fund. Theory Appl.*, 49(5):609–620, 2002.
- [19] P.A. Glendinning. Shilnikov chaos, Filippov sliding and boundary equilibrium bifurcations. *Unpublished.*, 2017.
- [20] D.J.W. Simpson. *Bifurcations in Piecewise-Smooth Continuous Systems.*, volume 70 of *Nonlinear Science*. World Scientific, Singapore, 2010.
- [21] M. di Bernardo, A. Nordmark, and G. Olivar. Discontinuity-induced bifurcations of equilibria in piecewise-smooth and impacting dynamical systems. *Phys. D*, 237:119–136, 2008.
- [22] F. Della Rossa and F. Dercole. Generalized boundary equilibria in n -dimensional Filippov systems: The transition between persistence and nonsmooth-fold scenarios. *Phys. D*, 241:1903–1910, 2012.
- [23] D.J.W. Simpson, D.S. Kompala, and J.D. Meiss. Discontinuity induced bifurcations in a model of *Saccharomyces cerevisiae*. *Math. Biosci.*, 218(1):40–49, 2009.
- [24] D.J.W. Simpson. Dimension reduction for slow-fast, piecewise-smooth, continuous systems of odes. Submitted to: *SIAM. J. Appl. Dyn. Sys.*, 2018.
- [25] E.D. Sontag. *Mathematical Control Theory*. Springer-Verlag, New York, 1998.
- [26] D.J.W. Simpson. Border-collision bifurcations in \mathbb{R}^n . *SIAM Rev.*, 58(2):177–226, 2016.
- [27] M. Guardia, T.M. Seara, and M.A. Teixeira. Generic bifurcations of low codimension of planar Filippov systems. *J. Differential Equations*, 250:1967–2023, 2011.
- [28] D.J.W. Simpson. Grazing-sliding bifurcations creating infinitely many attractors. *Int. J. Bifurcation Chaos*, 27(12):1730042, 2017.
- [29] V. Carmona, E. Freire, E. Ponce, and F. Torres. The continuous matching of two stable linear systems can be unstable. *Disc. Cont. Dyn. Sys.*, 16(3):689–703, 2006.

- [30] D.J.W. Simpson. The instantaneous local transition of a stable equilibrium to a chaotic attractor in piecewise-smooth systems of differential equations. *Phys. Lett. A*, 380(38):3067–3072, 2016.
- [31] P. Glendinning and C. Sparrow. Local and global behavior near homoclinic orbits. *J. Stat. Phys.*, 35(5-6):645–696, 1984.
- [32] N.K. Gavrilov and L.P. Šil’nikov. On three-dimensional dynamical systems close to systems with a structurally unstable homoclinic curve I. *Mat. USSR Sb.*, 17:467–485, 1972.